Phase Retrieval-Based Coherent Receivers: Signal Design and Degrees of Freedom

Elaine S. Chou, Hrishikesh Srinivas, *Graduate Student Member, IEEE*, and Joseph M. Kahn, *Fellow, IEEE*

(Invited Paper)

***Abstract*—Kramers-Kronig (KK) detection exploits properties of minimum-phase, single-sideband signals to recover the phase of a signal from its intensity. It offers many of the benefits of standard coherent detection, while not requiring a local oscillator, quadrature hybrid, or balanced photodiodes. Adding a carrier to a transmitted signal to render it minimum-phase, however, causes a power penalty for KK detection relative to standard coherent detection. We study the mutual information (MI) achieved by KK detection and the impact of signal and system design parameters, including excess bandwidth, carrier-to-signal power ratio, modulation order, probabilistic shaping, and chromatic dispersion, making comparisons to standard coherent detection and standard direct detection. We study the effective degrees of freedom for KK detection, confirming that it tends towards unity at high signal-to-noise ratio (SNR), supporting the classification of KK detection as coherent detection. At low SNR, however, KK detection is outperformed by standard direct detection in terms of MI per symbol. This study focuses on the fundamental performance of the detection methods under comparison, by numerically approximating ideal continuous-time signals and signal processing operations. The results and conclusions reported here will be constrained, in practice, by limitations of practical implementation, including those addressed in the Discussion section.**

***Index Terms*—Coherent detection, data center links, optical receivers.**

I. Introduction

OPTICAL fiber communication systems have relied on the high spectral efficiency and sensitivity of coherent detection to meet increasing demands for capacity. Coherent detection recovers the full electric field of a signal by measuring its two field quadratures (equivalently, its magnitude and phase) in two polarizations, maximizing the degrees of freedom of the information-bearing optical channel [1]. In standard coherent (SC) detection, widely used in long-haul systems, a strong local oscillator (LO) laser provides a phase reference for down-converting the signal at a receiver. The high cost and power consumption of such a receiver, which includes the LO laser, 90° optical hybrids, and high-speed digital signal processing (DSP) [2], has hindered its adoption in data center systems, which have traditionally used simpler intensity modulation/direct detection schemes that achieve lower spectral efficiency. Kramers-Kronig (KK) receivers, which implement coherent detection while avoiding complex receiver optics by performing direct detection followed by digital phase retrieval, show potential for scaling the capacity of data center systems. KK detection, as an intermediary between SC detection and standard direct (SD) detection, has therefore been studied in numerous experiments and theoretical analyses since its introduction by Mecozzi *et al.* [3], [4].

Although coherent detection can support and is used in links with much higher bit rates and transmission reach than direct detection, the decreasing cost of coherent detection and the increasing bit rate demands on data center links is creating potential overlap between the application of coherent and direct-detection links. As data center links scale beyond 400 Gb/s, chromatic dispersion (CD) creates challenges for direct-detection links even at moderate transmission reach, restricting the optical spectrum usable for wavelength-division multiplexing (WDM) near the zero-dispersion wavelength at 1310 nm and requiring increased spectral efficiency. Table I summarizes the fundamental differences between these three detection methods. Beyond these, other differences help define the application space for each method. All three detection methods are compatible with WDM, but KK detection and SD detection require higher bandwidth per channel owing to the minimum-phase condition and lack of nonnegative bandlimited root-Nyquist pulses, respectively. KK detection requires higher-bandwidth electrical components because of spectral broadening by a factor of two during intensity detection. SC detection can additionally be used in multicarrier transmission multiplexed in fiber modes and electric field polarizations. Multiplexing in spatial and polarization modes with KK detection is possible in principle, but is complicated in practice, as we discuss below. For a single-mode fiber (SMF) link, SC detection requires an LO laser, quadrature hybrid, and balanced photodiodes, in addition to two digital-to-analog converters (DACs) and two analog-to-digital converters (ADCs) in each polarization and wavelength channel to utilize the two signal quadratures, whereas SD detection requires one DAC and ADC each, and KK detection requires two DACs and one ADC at double the bandwidth and sampling rate.

In KK coherent detection, the phase $\varphi(t)$ of a band-limited signal $s(t)$ of overall bandwidth B is retrieved from the received

Manuscript received June 21, 2021; revised August 17, 2021, October 13, 2021, and November 16, 2021; accepted November 18, 2021. Date of publication November 25, 2021; date of current version March 2, 2022. This work was supported in part by the Maxim Integrated and in part by the Inphi Corporation (now part of Marvell Technology, Inc.). *(Corresponding author: Elaine S. Chou.)*

The authors are with E. L. Ginzton Laboratory, Department of Electrical Engineering, Stanford University, Stanford, CA 94305 USA (e-mail: eschou@stanford.edu; hrishsri@stanford.edu; jmkahn@stanford.edu).

Color versions of one or more figures in this article are available at https://doi.org/10.1109/JLT.2021.3130651.

Digital Object Identifier 10.1109/JLT.2021.3130651

TABLE I
DETECTION METHODS

Detection Method	Acronym	Description	Key Components for One Polarization	Decision Variable(s)	Classification
Standard direct	SD	Simple direct detection	Photodiode	Intensity	Noncoherent
Standard coherent	SC	LO-based downconversion and phase synchronization	LO laser, quadrature hybrid, balanced photodiodes, analog or digital phase synchronization	Field quadratures	Coherent
Kramers-Kronig	KK	Direct detection and phase retrieval	Photodiode, digital phase retrieval	Field quadratures derived from intensity and phase	Coherent

TABLE II
SIMULATION PARAMETERS

Parameter	Symbol	Value(s)
Symbol rate	R_s	64 GBaud
Oversampling rate	r_{os}	64
Modulation order	M	4, 16, 64
Excess bandwidth	β	0.01
Carrier-to-signal ratio	CSPR	optimized
Probabilistic shaping	λ	0

intensity $i(t) = |x(t)|^2$ via the Hilbert transform $\mathcal{H}\{\cdot\}$ as

$$\varphi(t) = \mathcal{H}\{\log \sqrt{i(t)}\}, \tag{1}$$

which is unique if the received signal $x(t)$ satisfies a minimum-phase condition [4]. This condition is enforced in practice by adding an unmodulated carrier E_0 at a band edge:

$$x(t) = E_0 + s(t)e^{j\pi Bt}. \tag{2}$$

The minimum-phase condition is satisfied if the unmodulated carrier shifts the information-bearing signal away from the origin of the complex plane sufficiently that time trajectories of the signal $x(t)$ do not encircle it. In this case, the original signal can then be recovered as

$$s(t) = \left(\sqrt{i(t)}\, e^{j\varphi(t)} - E_0\right) e^{-j\pi Bt}. \tag{3}$$

The potential for KK detection to achieve high capacity using simple optics is of particular interest in inter-data center and campus-wide links, which may be up to hundreds of kilometers in length, with industry standards up to 120 km in length [5]. In these links, even without the gain of a strong LO during optical-to-electrical downconversion, KK receivers may use optical amplification to boost receiver sensitivity, achieving amplified spontaneous emission (ASE) noise-limited performance [2]. Experimental demonstrations of KK detection are summarized in Table II of [2]. Transmission at 400 Gb/s over a record reach of 560 km has been achieved recently using a KK receiver with modified transmitter DSP and probabilistic shaping (PS) [6]. In concert, power consumption [7], upsampling [8], [9], analog methods for reducing error rates [10], [11], and DSP complexity [12] have been the subject of ongoing studies. The benefit of PS to KK detection has been studied numerically for specific values of the carrier-to-signal power ratio (CSPR) in [13].

In this paper, we review the fundamentals of KK detection, then address issues complementary to those examined in the prior work, comparing its performance to SC detection and SD detection. We focus on studying the fundamental performance of the detection methods, as opposed to the impact of implementation constraints, by numerically approximating ideal continuous-time signals and signal processing operations. Therefore, the specific values obtained by optimization in this study will change when other system limitations are accounted for. For example, in a system with limited ADC bandwidth or DSP oversampling rate, higher CSPR will be needed to counter the effects of filtering and lower sampling rate, and the optimal excess bandwidth will be lower to accommodate the ADC bandwidth. Expanding on the results of [14], we study signal design for KK detection, jointly optimizing the CSPR and the PS parameter as a function of the signal-to-noise ratio (SNR) and fiber CD. We find that optimized values of the PS parameter for KK detection differ substantially from those for SC detection and that CD causes SNR penalties for KK detection at typical inter-data center link lengths. We compare the information-theoretic metrics of mutual information (MI) and effective degrees of freedom (EDOF) for KK, SC, and SD detection. We verify that the KK receiver is a coherent receiver at high SNR, but find it is outperformed by SD detection at low SNR.

The remainder of this paper is structured as follows. Section II describes the system designs studied, the analytical and numerical methods used, and the information-theoretic metrics of MI and EDOF employed. It also discusses the optimal transmitted signal distribution for KK detection. Section III describes the optimization of signal parameters, including CSPR, PS parameter, and excess bandwidth; explains how these parameters are affected by CD; and presents the system performance obtained, in terms of MI or EDOF. Practical considerations, such as bandwidth limitations and oversampling considerations, are reserved for Section IV, which also discusses the implications and limitations of this study and directions for future work. Section V concludes the paper.

II. SYSTEM AND SIMULATION METHODOLOGY

The system under study is a single-polarization, amplified optical link, with an unmodulated carrier added at the transmitter for KK detection. KK detection, as originally proposed, can be implemented with the carrier added at either the transmitter or receiver side. Most studies, however, have added the carrier at the transmitter [8], [15]–[18], using amplification to compensate for link losses, which is necessary to support high data rates without the gain provided by a strong LO. Although we focus mainly on systems that add the carrier at the transmitter, in Section IV we discuss systems that add the carrier at the receiver.

A. System Description

Single-polarization waveforms at a wavelength of 1550 nm and a symbol rate of $R_s = 64GBaud$ are simulated, with

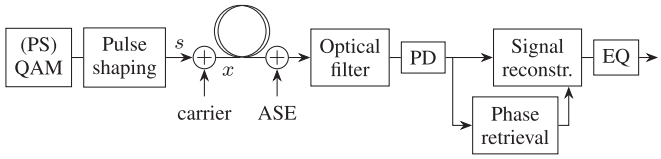

Fig. 1. Block diagram of a coherent optical link using KK detection with the unmodulated carrier added at the transmit side. The signal undergoes QAM modulation with optional probabilistic shaping (PS), followed by pulse shaping, carrier addition, fiber propagation, amplification that adds ASE noise, photodetection (PD), phase retrieval and signal reconstruction, and finally equalization (EQ) and matched filtering.

symbols drawn from a square quadrature amplitude modulation (QAM) constellation of varying orders. PS using a Maxwell-Boltzmann (MB) distribution [19] is optionally applied to the QAM sequence. The symbols are modulated by pulses whose Fourier transform is a root-raised cosine (RRC) with excess bandwidth β. An oversampling rate of 64 is used in this study to approximate continuous time. For accurate signal reconstruction free of aliasing, a KK receiver requires a minimum ADC oversampling rate of 2, with digital upsampling before KK signal processing by a factor of 3 [4], resulting in a final oversampling rate of 6, which yields nearly ideal performance if the CSPR is sufficiently high. An unmodulated carrier is added at the low-frequency band edge of the RRC-modulated signal, $R_s(1+\beta)/2$ away from the signal's center frequency, to satisfy the minimum-phase condition needed for the Hilbert transform relation between log-magnitude and phase used in phase retrieval to hold. The strength of the carrier is set by the CSPR, which is the unmodulated carrier power P_c divided by the modulated signal power P_s. The signal is propagated through standard SMF.

At the receiver, an optical amplifier generates ASE noise modeled by signal-independent additive white Gaussian noise (AWGN). The SNR is defined as the total signal power $P_s + P_c$ divided by the noise power with one-sided power spectral density N_0 in a bandwidth equal to the symbol rate R_s, and is given by

$$\begin{aligned}\text{SNR} &= \frac{P_s + P_c}{N_0 R_s} \\ &= \frac{P_s}{N_0 R_s}\left(1 + \frac{P_c}{P_s}\right) \\ &= \text{SNR}_{\text{sig}}(1 + \text{CSPR}),\end{aligned} \tag{4}$$

where SNR_{sig} is the SNR if carrier power is not included in total signal power.

The amplified optical signal is filtered by an ideal rectangular bandpass filter of bandwidth $R_s(1+\beta)$ and passed to the KK receiver for direct detection and phase retrieval. A practical filter will have a more gradual cutoff and leave some guard band, but the ideal filter provides conditions most favorable to the KK receiver while decoupling receiver performance from filter design. Finally, after CD compensation and matched filtering, the signal is sampled to produce the received symbol sequence.

The block diagram of a coherent link using KK detection with the carrier added at the transmitter is shown in Fig. 1. One photodiode is used to detect the optical intensity, from which the phase is retrieved under the assumption of minimum phase. The intensity and retrieved phase are used to reconstruct the signal's two quadrature components, after which equalization and matched filtering are performed.

B. Parameters and Metrics

The system parameters varied in this study are the QAM modulation order, excess bandwidth of the root-raised cosine pulse, CSPR, PS parameter, fiber length, and SNR. Table II summarizes the system parameters used in simulation. We simulate square QAM constellations of order 4, 16, and 64. Increasing the excess bandwidth of the root-raised cosine pulse allows more abrupt transitions from one QAM symbol to the next. The excess bandwidth is fixed to 0.01 when not under study for optimization. CSPR is a parameter unique to KK detection. In all results shown, it is optimized, unless a specific CSPR value is stated. Both SC and KK detection benefit from PS of the QAM constellation. When PS is used, the probability of a signal point i at distance r_i from the origin is given by the MB distribution

$$p_i = \frac{e^{-\lambda |r_i|^2}}{\sum_j e^{-\lambda |r_j|^2}}, \tag{5}$$

where an optimal value of the parameter λ is chosen at each SNR. In these studies, PS is not employed when other parameters are under investigation, but its optimization jointly with CSPR and excess bandwidth is considered for KK detection signal design.

We quantify system performance by capacity per symbol, estimating MI [20] per symbol (b/symbol) from the transmitted and received symbol sequences, assuming an auxiliary channel whose output, conditioned on its input, is independent over time [21]. A Gaussian noise distribution cannot be assumed because at low CSPR, phase retrieval errors introduce noise that deviates from a Gaussian distribution, so conditional probability distributions of the channel are estimated by binning symbols into two-dimensional histograms with optimized bin sizes [22].

In contrast to long-haul optical fiber links with dense frequency grids, data center links typically have more relaxed channel spacing requirements. Because KK receivers require single-sideband (SSB) signals to satisfy the minimum-phase condition, WDM channels must be cleanly separable by optical filtering, increasing the required channel spacing compared to SC detection. Because the channel spacing significantly exceeds the symbol rate and the symbol rate is constrained by electronic and photonic components, capacity in bits per symbol may be a more suitable metric than spectral efficiency in bits per second per Hz. Using capacity in bits per symbol as a performance metric also facilitates comparison to SD detection, for which band-limited non-negative root-Nyquist pulses do not exist [23].

Generalized mutual information (GMI) is often used to predict achievable rates on channels employing the soft-decision binary forward error correction (FEC) common in optical communication links [24], but we employ symbol-wise MI because it is more fundamental and is not constrained to bit-interleaved modulation. Additionally, when PS and FEC are optimized jointly, the optimal code rate typically exceeds 0.7 [25]; at such high code rates, the MI versus post-FEC error rate curves are consistent

between square QAM constellations of different orders [24], indicating that MI is a good metric for link performance.

A second metric presented in this paper is EDOF [26]. In a channel that can potentially convey multiple information streams in different physical variables, EDOF quantifies the number of independent parallel channels, i.e., dimensions, actively contributing to communication. It does so by studying the effect of increasing the input signal power on the capacity. In an AWGN channel with a single transmission mode, the capacity is $C = \log(1 + \text{SNR})$, and as SNR increases, the capacity increase resulting from an increase in signal power by a factor of $G = 2^{\delta}$ approaches

$$\lim_{\text{SNR}\to\infty} \log(1 + G \times \text{SNR}) - \log(1 + \text{SNR}) = \log G.$$

Correspondingly, the capacity of a system equivalent to EDOF independent parallel channels should increase by EDOF $\times$ $\log G$, so the EDOF of a channel at transmit power ρ is defined as [26]

$$\begin{aligned}\text{EDOF}\,(\rho) &= \frac{d}{d\delta} C(2^{\delta}\rho)\bigg|_{\delta=0} \\ &= \frac{dC}{dP} 10\log_{10} 2, \end{aligned} \tag{6}$$

where $P = 10\log_{10}\rho$ is the transmit power in dB. Note that in contrast to a constant scale factor that multiplies the log function in the capacity expression, EDOF is a function of SNR. In the low-SNR regime, EDOF is power limited, whereas at high SNR it is limited by the number of dimensions, so EDOF captures how incremental efficiency varies as a function of SNR. A coherent system transmitting in one polarization that fully utilizes one complex dimension, or two real dimensions, has an EDOF that approaches 1 at high SNR, whereas a corresponding direct detection system's EDOF is upper bounded by 1/2. For example, with SC detection, the EDOF follows

$$\text{EDOF}_{\text{sc}} = \frac{1}{1 + \text{SNR}^{-1}}, \tag{7}$$

which has an asymptote at 1 as SNR approaches infinity. Thus, EDOF can be used to confirm that the performance of KK detection is consistent with coherent detection.

For a fixed, finite constellation order, as the SNR is increased, EDOF will rise to a maximum and then decrease to zero at high SNR when the channel capacity reaches the constellation entropy. Therefore, in estimating EDOF, we evaluate MI using QAM orders as high as 4096. Owing to computational limitations, MI computations for estimating EDOF use a Gaussian noise approximation. In an ASE noise-limited system, SNR is linearly proportional to transmit power, so EDOF is proportional to the slope of the capacity curve plotted against SNR expressed in dB.

C. Transmitted Signal Distribution

In this section, we discuss the capacity-achieving transmitted signal distribution for KK detection and how to approximate it in practice by a finite-order QAM constellation with PS.

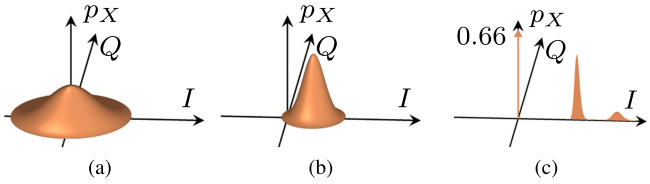

Fig. 2. Idealized capacity-achieving marginal probability density functions (pdf's) p_X of the transmitted signal field quadratures per complex dimension (symbol interval) considered in this study for (a) standard coherent detection, (b) KK coherent detection with 5 dB CSPR, and (c) standard direct detection at 5 dB SNR, drawn on the same scale. The pdf's (a) and (c) assume a frequency origin at the center of the modulated data-bearing signals, whereas the pdf (b) assumes a frequency origin at the unmodulated carrier. For clarity, the pdf in (c) assumes a non-negative, real signal; an arbitrary phase can be included without affecting mutual information. I: in-phase, Q: quadrature.

Throughout this section, we assume that phase-retrieval errors have negligible impact on MI.

Fig. 2 plots the idealized, continuous-valued capacity-achieving transmitted signal distributions for the three detection methods considered. Whereas SC detection and KK detection can exploit both the in-phase and quadrature dimensions, SD detection measures only intensity, so it is restricted to a single dimension. For SC detection, the optimal distribution is a zero-mean complex circular Gaussian distribution with variance equal to the signal power [20]. For KK detection, this Gaussian distribution is shifted away from the origin by the unmodulated carrier. For both detection methods, the Gaussian distribution can be approximated in practice by a finite-order QAM constellation that is shaped by an MB distribution. The capacity-achieving distribution for SD detection, shown in Fig. 2(c), is discussed in Section III-E below.

It is easily shown that the capacity-achieving distribution for KK detection is the same as for SC detection, except for the unmodulated carrier that shifts the signal away from the origin. We consider a modulated signal s with power P_s represented by the random variable S to which a carrier with power P_c is added, producing a composite signal x with power P represented by the random variable X. The capacity-achieving input distribution satisfies a constrained optimization

$$\begin{aligned}&\max._{P_X} I(X;Y) \\ &\text{s.t. } P \le P_{\max}. \end{aligned} \tag{8}$$

Addition of the carrier preserves MI, i.e., $I(X;Y) = I(S;Y)$ for channel output Y and either X or S taken as the channel input. In general, $P \ge P_c + P_s$, because of cross terms between the signal and carrier in the squaring operation. In a system using KK detection, however, there is no frequency overlap between the carrier and the SSB signal, so there are no cross terms. Hence, constraining the total power to $P \le P_{\max}$ is equivalent to constraining the signal power to $P_s \le P_{\max} - P_c$. Combining the observations that adding the carrier does not affect MI and that it adds a constant power P_c to the composite signal x, the optimization in (8) is equivalent to

$$\begin{aligned}&\max._{P_S} I(S;Y) \\ &\text{s.t. } P_s \le P_{\max} - P_c, \end{aligned} \tag{9}$$

and the capacity-achieving distribution can be determined without considering the effect of the carrier, aside from the decreased power available for the signal. As long as the carrier amplitude is sufficiently high to ensure accurate phase retrieval (i.e., the minimum-phase condition is satisfied), KK detection will recover the transmitted signal with AWGN, as in SC detection. The optimization in (9) is unchanged from a system using SC detection, so the optimal transmit probability distribution P_X is a complex circular Gaussian distribution shifted away from the origin.

It may appear that in KK detection, adding the carrier breaks the symmetry of the signal, such that an asymmetric probability distribution may outperform a symmetric distribution, but because the carrier is added at a band edge of the signal, any asymmetries in the signal constellation are averaged out over time. We can visualize the rotation of a signal constellation $s(t)$ with symbol rate R_s and excess bandwidth β after a carrier E_0 is added at the lower band edge. Referenced to the carrier frequency, the received signal can be written as

$$x(t) = E_0 + s(t)e^{j\pi(1+\beta)R_s t}, \tag{10}$$

where the signal constellation is rotating about its center at a rate of $(1+\beta)R_s/2$. If there is no excess bandwidth, symbol-spaced sampling of the signal at $t = k/R_s$ yields

$$x[k] = E_0 + s[k]e^{jk\pi} = E_0 + s[k](-1)^k. \tag{11}$$

Hence, the constellation rotates by π in each symbol period, and half of the samples are inverted with respect to their original location in the complex plane. When using arbitrary nonzero excess bandwidth, each point in the transmitted signal is mapped in the sampled signal to equally spaced points on a circle centered at E_0, which lie at different distances from the origin and overlap with samples from other transmitted signal points. If instead we reference the signal to its center frequency, then the signal becomes

$$x_c(t) = E_0 e^{-j\pi(1+\beta)R_s t} + s(t). \tag{12}$$

In this frame of reference the signal constellation itself does not rotate but is translated around a circle by the carrier that is rotating around the origin. This effect causes the distance from the origin to each constellation point to change with time. Both visualizations lead to the conclusion that asymmetry cannot be exploited.

In practice, a continuous-valued capacity-achieving distribution is approximated by a discrete-valued finite-order constellation, using PS to maximize MI subject to an average-power constraint. By selecting low-power inner points with higher probabilities than high-power outer points, PS decreases the average power of a constellation. PS also decreases the entropy of a constellation, but can improve power efficiency on channels with SNR too low to support the full entropy of a uniform constellation.

PS was first studied for Gaussian channels [19], [27], [28], and this original formulation has been applied extensively in recent years to optical systems using SC detection. PS has also been studied for optical systems using SD detection, including those limited by thermal noise [29] and those limited by optical amplifier noise [30]. Although the KK receiver uses direct detection, it is a coherent receiver, and its capacity-achieving distribution is a shifted Gaussian, as explained above. When using a finite-order QAM constellation, the corresponding PS distribution is a shifted MB distribution [19], which has been used in studies of KK detection, e.g., [13].

III. Results

In addition to CSPR, which we optimize throughout this study (except when we state a specific value of CSPR), we study the effects of varying excess bandwidth, CD, and PS parameter. As we vary each parameter, we hold the remaining parameters fixed, unless we state otherwise. The default simulation conditions are back-to-back transmission with excess bandwidth $\beta = 0.01$ and no PS. In this section, we first study the effect of CSPR on KK receiver performance, discussing trends in CSPR as a function of SNR. Next, we perform joint optimization of CSPR and excess bandwidth, as well as CPSR and PS parameter, for SNRs ranging from -530 dB. We also study the performance penalty induced by CD when optimizing all three parameters of signal design. Our results focus on KK systems that add the unmodulated carrier at the transmitter; we discuss adding the carrier at the receiver in Section IV.

When performance is quantified by required electrical SNR at a given CSPR using KP4 FEC [31], clipping has been shown to enhance KK receiver performance in unamplified systems with CSPRs down to 6 dB in the presence of thermal noise, which can potentially cause detected intensity signals to become negative [10]. By contrast, in this work, we study ASE noise-limited systems with performance quantified by MI, where the optimized CSPR is often below 6 dB. Low CSPR is more of a limiting factor than noise in this work, and we observe no MI gain from clipping.

A. Carrier-to-Signal Power Ratio

In order for KK detection to accurately reconstruct phase from intensity, a carrier must be added to the signal. More precisely, KK phase retrieval relies on the assumption that the transmitted signal is minimum-phase. A necessary and sufficient condition for minimum phase of SSB signals is that the time trajectory in the complex plane does not encircle the origin [4]. As CSPR increases, the trajectory shifts away from the origin and the minimum-phase condition holds more robustly, but a power penalty is incurred.

As observed in previous work, e.g., [17], at high CSPR, the total SNR penalty is roughly $\Delta\text{SNR} \approx 1 + \text{CSPR}$, but as CPSR decreases, errors in phase retrieval contribute to an SNR penalty beyond the power required by the unmodulated carrier. Thus, at each SNR, there is an optimal CSPR, which balances the power penalty of the unmodulated carrier against that caused by phase-retrieval errors. The decomposition of the SNR penalty into phase-error and carrier-power contributions is shown in Fig. 3. As the SNR increases, to take full advantage of the reduced noise, the optimal CSPR increases to improve phase-retrieval accuracy. At 30dB SNR, the CSPR optimized with respect to MI is about 7 dB and the SNR penalty stems entirely from carrier power;

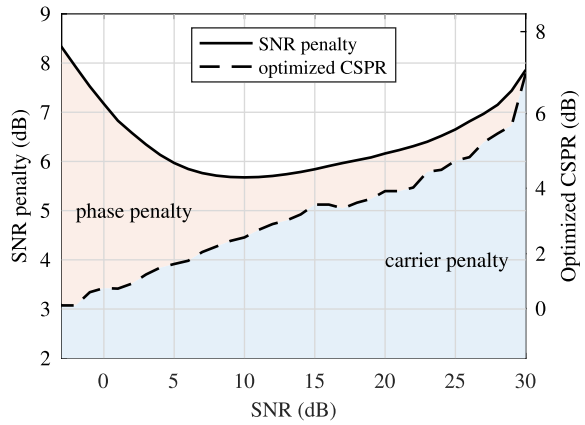

Fig. 3. SNR penalty of KK detection with respect to SC detection for uniform-probability 64-QAM in back-to-back transmission. The SNR penalty is split into phase-error and carrier-power components.

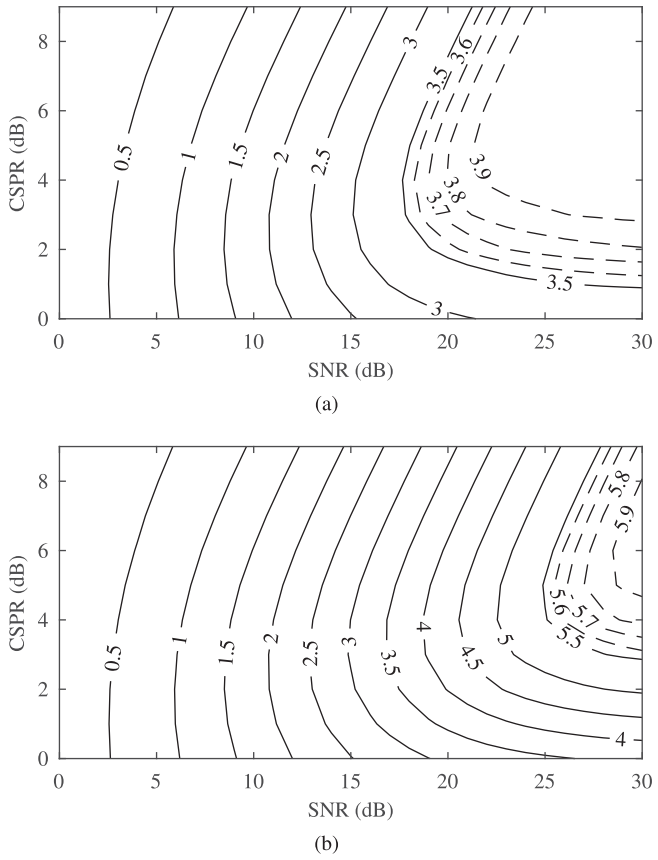

Fig. 4. Contours of MI as a function of CSPR and SNR for KK detection of uniform-probability a) 16-QAM and b) 64-QAM constellation with entropy of 4 and 6 b/symbol, respectively, in back-to-back transmission. Solid lines have 0.5 b/symbol spacing, and dashed lines have 0.1 b/symbol spacing.

at 15 dB SNR, the optimized CSPR drops to 3.5 dB and the SNR penalty is 5.8 dB, of which 5.1 dB is due to the carrier and the remaining 0.7 dB is due to phase-retrieval errors. Supporting low CSPRs that introduce more noise requires stronger FEC and consideration of phase error effects during equalization.

Fig. 4 plots contours of MI as a function of CSPR and SNR for 16-QAM and 64-QAM transmission. Vertical and horizontal cross sections of the contour plot provide insight to the dependence of MI on CSPR and SNR, respectively. As the CSPR increases, eventually minimum phase-violating events become so infrequent that the phase-error penalty is almost zero, and any further increase of CSPR only decreases $\mathrm{SNR}_{\mathrm{sig}}$ with no benefit. Let us designate the lowest CSPR at which the phase-error penalty vanishes as CSPR_0. The constrained capacity of a channel transmitting a finite-order constellation is bounded by the transmit constellation's entropy, and beyond a certain SNR value $\mathrm{SNR}_{\mathrm{sat}}$, the MI increase is effectively zero. Then, if the channel SNR is high enough, there is a range of CSPR values $\mathrm{CSPR}_0 \leq \mathrm{CSPR} \leq \mathrm{CSPR}_1$, where

$$\mathrm{CSPR}_1 = \frac{\mathrm{SNR}}{\mathrm{SNR}_{\mathrm{sat}}} - 1, \tag{13}$$

for which the MI is almost flat, at a value equal to the entropy of the transmit constellation, as seen in the upper-right region of Fig. 4(a). At SNRs below 15 dB, varying CSPR or SNR by 5 dB causes MI to change by up to 1 b/symbol. In contrast, as the channel capacity approaches the entropy of the transmit constellation, the dependence of MI on both CSPR and SNR weakens, and there is less than 0.1 b/symbol change in MI over the region spanning 24 to 30 dB SNR and 3 to 8 dB CSPR. Thus, at high SNR, CSPR optimization can be performed loosely without significant MI penalty.

A square M-QAM constellation has a peak-to-average power ratio (PAPR)

$$\mathrm{PAPR} = \frac{3\left(\sqrt{M}-1\right)^2}{M-1}, \tag{14}$$

which has a minimum of 1 at $M = 4$ and approaches 3 as M increases. The PAPR is the minimum CSPR required to shift the constellation completely away from the origin, neglecting the effect of overshoot in the signal trajectory. Therefore, lower-order constellations require lower CSPR values, and the optimized CSPR also plateaus at lower values. The easiest case to study is 4-QAM, where a plateau in optimized CSPR is observed around 4 dB when the SNR is above 15 dB, roughly coinciding with the SNR range where the 4-QAM constellation entropy saturates at 2 bits per symbol.

B. Excess Bandwidth

The root-raised cosine pulse shape is a root-Nyquist pulse that trades excess signal bandwidth for reduced overshoot in transitions between QAM symbols; increasing excess bandwidth enables operation at lower CSPR. At either low SNR or high CSPR, however, increasing the excess bandwidth can cause MI per symbol to decrease, because the corresponding increased optical filter bandwidth passes more noise. Although in SC detection matched filtering negates the effect of increased filter bandwidth, in KK detection, because phase retrieval occurs before electrical matched filtering, the excess noise can exacerbate phase errors and impair performance. Under conditions of high SNR and low CSPR, optimization of excess bandwidth

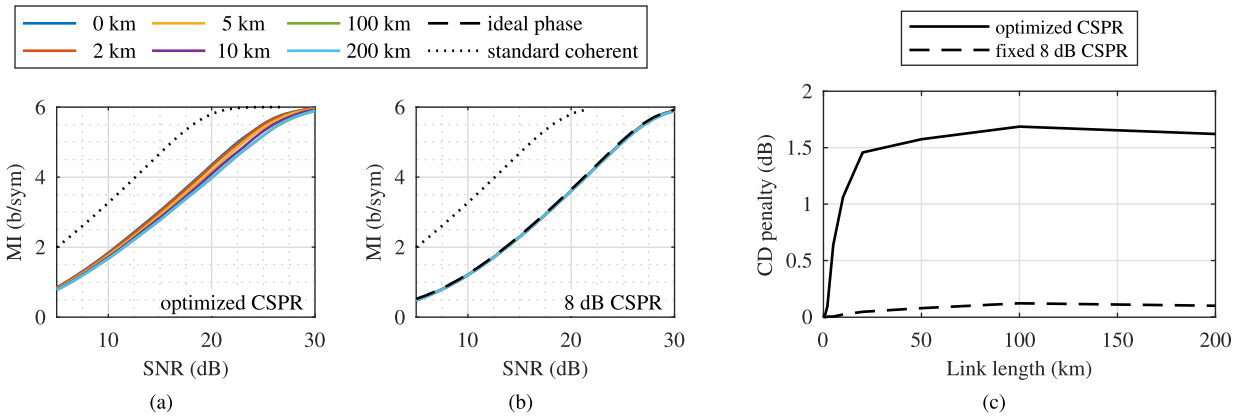

Fig. 5. Effect of chromatic dispersion on KK receiver performance for a system transmitting uniform-probability 64-QAM over standard SMF link lengths up to 200 km: MI vs. SNR with (a) optimized and (b) fixed 8 dB CSPR. (c) CD penalty of KK detection with optimized CSPR and with fixed 8 dB CSPR.

can increase MI. When excess bandwidth is optimized jointly with CSPR, however, a small capacity increase is obtained; for SNRs ranging from -530 dB, the maximum MI increase achieved with pulse shaping of a 64-QAM signal is 0.1 b/symbol (2.1%) at 25 dB SNR, and 0.09 b/symbol (2.4%) at 15 dB for 16-QAM, both requiring an excess bandwidth of 0.5. In this study, a small default excess bandwidth of $\beta = 0.01$ is chosen to minimize component bandwidth requirements while avoiding the undesirable effects of ideal sinc pulses that have abrupt frequency cutoffs.

Most notably unique to KK detection with regard to excess bandwidth, if the excess bandwidth is exactly zero, then as previously noted in Section II-C (11), during one symbol period the symbol constellation rotates by a half revolution, so each constellation point is mapped to two possible locations in the complex plane during phase retrieval. In the noiseless case, phase errors $\Delta\varphi$ will cause the error after signal reconstruction using (3) to follow the two paths

$$e[n] = (s[n] \pm E_0)\left(e^{j\Delta\varphi[n]} - 1\right), \tag{15}$$

depending on whether n is even or odd, resulting in a noise distribution that is not Gaussian. With nonzero excess bandwidth, the effect of phase errors is more distributed over direction, so the capacity estimated using a Gaussian noise approximation becomes more accurate.

C. Chromatic Dispersion

To study the KK receiver's robustness against CD, we simulate transmission over standard SMFs up to 200 km in length. For a fiber with dispersion slope $S_0 = 0.092\,\mathrm{ps}/(\mathrm{nm}^2 \cdot \mathrm{km})$ and zero-dispersion wavelength $\lambda_0 = 1310\mathrm{nm}$, the dispersion parameter at 1550 nm is $D = 17.4\mathrm{ps}/(\mathrm{nm} \cdot \mathrm{km})$. As CD increases the memory length of the channel, the minimum block length over which the KK receiver performs phase retrieval increases proportionally. A 100-km fiber link accumulates around $t = 900\,\mathrm{ps}$ or 58 symbols of memory due to CD, which still allows for a KK computation window length sufficiently short that the phase noise from a laser with a 1-MHz linewidth $\Delta\nu$, with a variance of $\sigma^2 \approx 2\pi\Delta\nu t = 0.006 \ll 1$, is approximately constant over the entire window. For a fiber attenuation constant of 0.2 dB/km, 1 mW launch power, amplifier n_{sp} of 2.8, and a 64 GBaud signal at 1550 nm, the SNR after 100 km of fiber is 27 dB.

SC detection incurs no penalty for the CD simulated, as expected. Using KK detection at fixed, high CSPR values $(> 7\mathrm{dB})$ where the total SNR penalty is dominated by the extra carrier power, CD causes an SNR penalty of less than 0.1 dB and MI loss of less than $0.03\,\mathrm{b/symbol}$, as shown in Fig. 5(b), where MI curves for all fiber distances overlap with the ideal phase retrieval case. This result is consistent with the general observation that at high SNRs, after the carrier power penalty has been accounted for, KK receivers behave similarly to SC receivers. When the CSPR is optimized to maximize MI at each SNR, however, the presence of CD increases the required CSPR and ultimately leads to a 1.7-dB SNR penalty and 0.2-b/symbol MI loss at 27 dB after 100 km of fiber. Fig 5(a) plots the MI with optimized CSPR. The corresponding CD penalty of KK detection with optimized CSPR is plotted in the solid line of Fig. 5(c). The CD penalty accumulates quickly at shorter distances, but levels off at longer distances; there is almost no additional CD penalty when increasing the fiber length from 100 km to 200 km.

D. Probabilistic Shaping

When we use PS with KK detection, we jointly optimize the PS parameter λ and the CSPR to maximize MI. We first present results for back-to-back transmission before presenting the effect of CD on PS. In KK detection with back-to-back transmission, weaker PS is preferred compared to SC detection because PS increases the probability of lower-power constellation points, decreasing the average power and increasing the PAPR. Consequently, a higher carrier power is required to push the corner points sufficiently away from the origin to satisfy the minimum-phase condition. The trends of PS parameter λ with SNR for a 64-QAM constellation are shown in Fig. 6(a), and the resulting MI is shown in Fig. 7. As with other detection methods, there is weak dependence of MI on the PS parameter λ at low SNRs, where the MI for different constellation orders

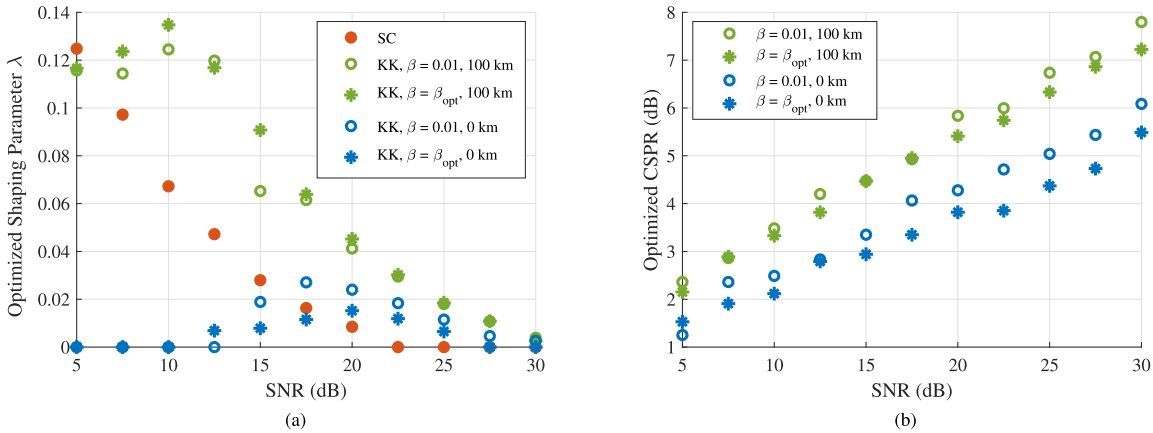

Fig. 6. Optimized (a) PS parameter λ and (b) corresponding CSPR vs. SNR for 64-QAM. Parameter values without CD in back-to-back transmission (0 km) are shown in blue, and those with CD from 100 km of standard SMF are shown in green. Parameter values optimized with fixed excess bandwidth $\beta = 0.01$ are shown as open circles, whereas those optimized jointly with excess bandwidth $\beta = \beta_{\text{opt}}$ are shown as stars. In (a), the optimized PS parameter for SC detection is shown as red filled circles for comparison.

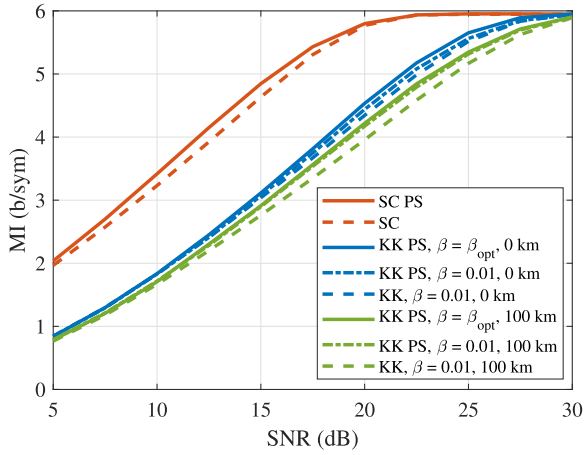

Fig. 7. MI vs. SNR for the KK and SC receivers for 64-QAM, with the optimized parameter values shown in Fig. 6. The SC receiver curves with optimized PS (solid) and without PS (dashed) are shown in red. The KK receiver curves without CD in back-to-back transmission (0 km) are shown in blue, and those with CD in 100 km of standard SMF are shown in green. Results are shown for three scenarios: both PS parameter λ and excess bandwidth β optimized (solid curves); λ optimized with fixed excess bandwidth $\beta = 0.01$ (dot-dashed curves); and no PS, i.e., $\lambda = 0$, with $\beta = 0.01$ (dashed curves). All KK receiver curves assume that CSPR is optimized either jointly with λ or alone without PS.

and distributions converges. In contrast to SC detection, where stronger shaping is needed to maximize MI as SNR decreases, for KK detection the optimal PS parameter peaks at SNRs between 15 and 20 dB, and at SNRs of 10 dB and below, uniform constellations ($\lambda = 0$) achieve the highest MI. The peaking in PS parameter is caused by the competing objectives of maintaining minimum phase and maximizing power efficiency, which favor points far from and close to the origin, respectively. Comparing Fig. 3 with Fig. 6(b) reveals that at SNRs between 15 and 25 dB, where PS does increase MI, the optimal CSPR is increased by PS.

Fig. 6(b) shows the increase in optimal CSPR with SNR in the case of 64-QAM, when CSPR is optimized jointly with PS parameter λ, and in the presence of CD, comparing back-to-back transmission in blue and transmission over 100 km of standard SMF in green. Also compared are the cases with fixed excess bandwidth $\beta = 0.01$ (open circles) and optimized excess bandwidth $\beta = \beta_{\text{opt}}$ (stars), as described in Section III-B. Optimizing excess bandwidth enables a slight reduction in the optimal CSPR. Fig. 6(a) shows the corresponding jointly optimized values of the PS parameter λ vs. SNR for KK detection, with values for SC detection shown as filled red circles for comparison.

Fig. 7 compares the MI of the SC receiver with PS (solid curves) and without PS (dashed curves) in red, and the KK receiver in each of the three cases shown: that with both PS parameter λ and excess bandwidth β optimized (solid curves); that with λ optimized with fixed excess bandwidth $\beta = 0.01$ (dot-dashed curves); and that with no PS ($\lambda = 0$), with $\beta = 0.01$ (dashed curves). All KK receiver curves assume CSPR is optimized at each SNR either jointly with λ as presented in Fig. 6 (solid and dot-dashed curves) or alone (dashed curves). The KK receiver in back-to-back configuration, whose results are presented as the blue curves at 0 km link length in Fig. 7, achieves increased MI from optimizing the PS parameter λ, shown by the open blue circles and stars in Fig. 6(a), for SNRs over about 15 dB. In the presence of CD, where the noise is rendered approximately Gaussian even down to low SNRs, stronger PS is observed to be optimal, as shown by the open green circles and stars in Fig. 6(a), and the optimization of PS is more similar to that for SC detection than for KK detection in the absence of CD, with the optimal λ increasing as SNR decreases, roughly following the same trend as for SC detection but with an SNR shift corresponding to the carrier power. Thus, using the same PS parameter as one would choose for SC detection with the same signal SNR after removal of the carrier power, SNR_{sig}, can result in capacity loss for short links, but the capacity loss is smaller for longer links with CD due to more similar PS parameter trends. The resulting improvement in MI from PS in the presence of CD is seen in Fig. 7 as the gap between the solid and dot-dashed green curves, and the dashed green

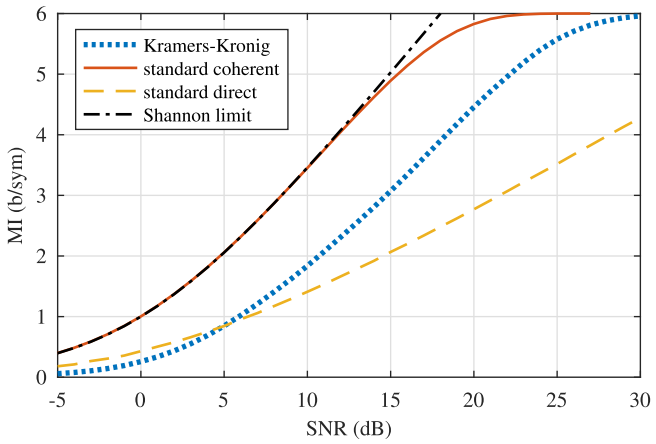

Fig. 8. MI vs. SNR for back-to-back transmission, comparing SC detection (red solid) and KK detection (blue dotted) using PS 64-QAM constellations, and SD detection (yellow dashed) using a 64-PAM constellation shaped by a capacity-achieving distribution.

curve, at 100 km link length. Optimization of excess bandwidth is seen to provide an additional improvement in MI, particularly for back-to-back transmission with no CD, as discussed in Section III-B. As shown in Fig. 7, optimizing excess bandwidth in conjunction with PS and CSPR in this case can increase MI by up to 0.2 b/symbol, with optimized excess bandwidth values ranging from 0.01 at low SNR to 0.5 at high SNR over 25 dB. In the presence of CD, the MI gain from optimizing excess bandwidth in addition to PS and CSPR is negligibly small and PS provides the majority of the improvement observed between the solid and dashed green curves.

In each case, optimizing the signal design parameters of CSPR, PS, and excess bandwidth can yield an increase in MI of up to 0.2b/symbol over the default conditions for KK detection, an increase comparable to that of PS applied to SC detection, albeit at higher SNR. To optimize performance, a transmitter–receiver pair may choose a value of λ from a look-up table depending on the link length and SNR, or may dynamically vary the value of λ to maximize the achievable bit rate.

E. Standard Direct Detection

Fig. 8 compares the MI achieved by SC detection, KK detection, and SD detection when nonequiprobable symbols are transmitted back-to-back. The SC and KK detection systems transmit 64-QAM shaped by an MB distribution, whereas the SD detection system transmits 64-PAM shaped by a capacity-achieving probability distribution.

The distribution for SD detection is obtained using the Arimoto algorithm [32] to numerically optimize input symbol probabilities over a channel with conditional probability density function (pdf) following a noncentral χ^2 distribution with two degrees of freedom [33]. The resulting transmit pdf's, like that shown in Fig. 2(c), comprise a discrete component of high probability at zero intensity, and a continuous distribution at positive intensity values. For purposes of illustration, the direct detection signal is assumed to be purely real, although any constant phase can be applied without affecting capacity. The half-Gaussian distribution obtained as the optimal shaping distribution in [30] relies on approximations valid at high SNR, and although nearly capacity-achieving at high SNR, is not identical to the capacity-achieving distribution shown in Fig. 2(c), differing noticeably at low SNR [33].

In simulation, uniformly spaced PAM constellations of order 64 are considered, with level scaling and probabilities optimized for each SNR. The transmit symbol constellations obtained are used in simulating a continuous-time SD detection system transmitting rectangular pulses filtered by a fifth order Bessel filter with optimized cutoff frequency. Optimized cutoff frequencies range from $1 \times R_s$ at -5 dB SNR to $1.6 \times R_s$ at 25 dB SNR. The simulated continuous-time SD detection system achieves an MI that is, on average, 5% lower than the capacity of a discrete memoryless channel estimated using the Arimoto algorithm.

Whereas the MI for KK detection roughly follows that of SC detection with a 5–7 dB SNR penalty, reaching a maximum of 6 b/symbol at around 30 dB SNR, the MI for SD detection rises more slowly, reaching only 4.3 b/symbol at 30 dB SNR. Fig. 8 also shows that the MI for SD detection exceeds that for KK detection at SNRs below 5 dB, although these SNRs are lower than in typical inter-data center links. Fig. 8 plots the MI for 64-ary constellations, but at SNRs below 5 dB, SD detection exhibits a negligible loss of MI when using more practical constellations, such as 4-PAM; using on–off keying results in a 0.1 b/symbol MI loss at 5 dB. The superior MI achieved by SD detection at low SNR is explained by the ability of SD detection to exploit the zero intensity level, which has the least noise. As shown in Fig. 2(c), at 5 dB SNR, more than half of the transmit probability for SD detection is in the zero intensity level. By contrast, the unmodulated carrier needed for KK phase retrieval pushes the probability distribution away from zero, as seen in Fig. 2(b), decreasing power efficiency. Intra-data center links, which are unamplified, will have lower SNRs than the inter-data center links considered in our ASE noise-limited model. In such thermal noise-limited systems, KK detection may perform worse than SD detection.

F. Effective Degrees of Freedom

Fig. 9 shows the EDOF achieved by SC detection, KK detection, and SD detection in back-to-back transmission. In evaluation of MI, SC detection and KK detection use M-QAM, $M \leq 4096$, which is shaped by an MB distribution, whereas SD detection uses M-PAM, $M \leq 1000$, which is shaped by the capacity-achieving distribution described in Section III-E. As expected, the EDOF for SD detection in Fig. 9 approaches 1/2 at high SNR, whereas the EDOF for SC detection follows (7) and reaches 1 at around 25 dB. At higher SNRs, the EDOF of KK detection approaches 1, as expected of a coherent receiver, although it remains below 0.95 even for SNRs above 35 dB. The EDOF of KK detection does not fully reach 1 because the optimal CSPR increases with SNR, so as the available power increases, a growing fraction is consumed by the carrier power rather than contributing to information transfer. At SNRs below

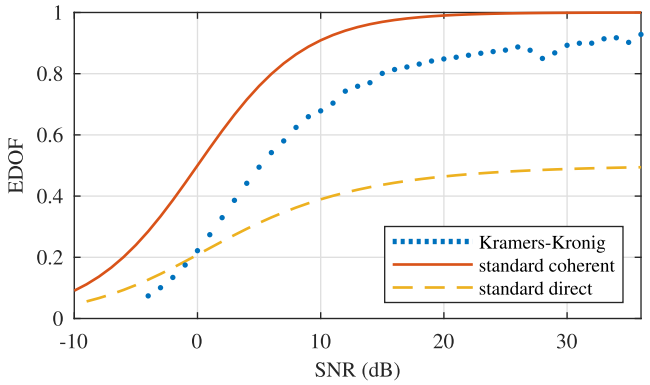

Fig. 9. EDOF for back-to-back transmission, comparing SC detection (red solid) and KK detection (blue dotted) using PS QAM and and SD detection (yellow dashed) shaped by a capacity-achieving distribution.

0 dB, the EDOF for KK detection is lower than that for SD detection, for reasons stated in Section III-E.

IV. Discussion

In this paper, we have compared the fundamental performance of KK, SC, and SD receivers for single-polarization signals. Here, we briefly address additional topics related to KK detection, including bandwidth and oversampling considerations, addition of the carrier at the receiver, and dual-polarization reception.

The most serious challenge for KK detection is that it requires significantly higher sampling rates and DSP complexity than SC detection, likely causing KK receivers to be limited by silicon circuit constraints. Both ADC bandwidth and DSP processing capability are limiting factors for the practical deployment of KK receivers. Whereas SC detection can achieve good performance with oversampling rates slightly higher than 1, KK detection requires a minimum oversampling rate of 2, owing to the squaring inherent in intensity measurement. Including excess bandwidth will place further strain on electrical components because of increased bandwidth requirements. Deployed systems will need to balance the increased MI from optimized excess bandwidth with the signal distortion from limited component bandwidths. Additionally, in real-time DSPs, high oversampling ratios are not feasible, so further performance degradation will be introduced.

In KK detection, the log operation causes additional spectral broadening, especially when the CSPR is low, because it amplifies intensity changes near the origin, introducing high frequency components. Thus, even with a minimum-phase signal, an insufficient sampling rate can introduce errors in phase retrieval, as shown analytically for a signal constructed with one frequency component in addition to the carrier [9]. Using FEC coding with 20% overhead, a CSPR of 6 dB minimizes the required SNR, requiring digital upsampling to at least 6 samples per symbol to approach ideal performance [17]. In this work, we employed a high oversampling rate for all detection methods to study the fundamental performance absent complexity constraints. Optimizing CSPR at each SNR balances the contribution of error sources, as discussed in Section III-A, so the error from sampling is small compared to other error sources such as ASE noise or violation of the minimum-phase condition. Lowering the ADC oversampling rate to 2 with a digital upsampling factor of 3 causes less than 0.03 b/symbol of MI loss over the range of SNRs studied here when CSPR is optimized. Approximations of the KK algorithm have been proposed to eliminate the need for digital upsampling [4], [8] and reduce DSP complexity [12], [34]. The approach outlined in [4] results in minimal visible signal degradation, and that of [8] increases the optimal CSPR by 2 dB and degrades the receiver sensitivity by 0.4 dB after 80 km transmission while decreasing DSP complexity compared to a conventional KK receiver by 80%.

In the KK receiver implementation studied here, the carrier is added at the transmitter, which is the most common choice for KK implementation, in part, because it facilitates aligning the signal and carrier polarizations [8], [12], [15]–[18]. The carrier can be generated by a separate laser, or as a virtual carrier in the digital domain [35]. Allocation of transmit power to a carrier entails a significant SNR penalty that must be taken into account when assessing capacity for a given power budget. The carrier power is the most significant source of penalty in KK receivers. Alternative KK implementations, in which a relatively weak carrier (a "weak LO") is added at the receiver, have also been considered [2], [12], [36]. When the carrier is added at the receiver, it can be made as strong as necessary to satisfy the minimum-phase condition without increasing the transmit power, and the performance of KK detection can approach that of SC detection. Whereas most of the performance differences between KK and SC detection are removed if a weak LO is added at the receiver, the weak LO requires accurate frequency stabilization, much like the strong LO for SC detection. In addition, the weak LO must be matched in polarization to the received signals. Consequently, although KK detection using a weak LO does not require the quadrature hybrids or balanced photodiodes used for SC detection, in practical terms, SC detection using a strong LO may be a better option than KK implemented with a weak LO at the receiver.

KK detection, as a form of coherent detection, fundamentally enables compensation of all linear effects, including polarization rotation that causes crosstalk between dual-polarization signals. However, the embodiment of KK detection we have studied in this paper, in which the carrier is added at the transmitter, is not suited for dual-polarization reception without modification. If two independent minimum-phase signals are polarization-multiplexed and transmitted through a fiber, the received polarization components are not guaranteed to be minimum-phase [2]. Several options adapting KK receivers to polarization-multiplexed signals exist, but they require adding optical components, such as a LO laser or optical polarization controller, to the receiver [2], [36]. These compromise the KK receiver's advantage of using simpler optical components than a SC receiver. Important directions for further research include polarization-demultiplexing schemes and the impact of polarization effects, such as polarization-mode dispersion or polarization-dependent loss/gain, on signal design for KK receivers [4], [36], [37].

V. Conclusion

A KK receiver best approaches its potential as a coherent receiver at high SNR, where the performance penalty relative to a SC receiver stems primarily from the unmodulated carrier needed to avoid phase-retrieval errors, quantified by the CSPR. At high SNR, the KK receiver achieves an EDOF approaching 1, yielding nearly two real dimensions per symbol, supporting its classification as a coherent receiver; however, it incurs an SNR penalty of about 7 dB compared to SC detection. The KK receiver benefits from joint optimization of the CSPR and PS parameter. As the SNR decreases, the optimal CSPR decreases, whereas the phase-error penalty increases. Although the KK receiver uses the same PS distribution as a standard coherent receiver, in the absence of CD, KK favors weaker PS than SC detection. In the presence of CD, KK detection incurs an additional SNR penalty of 1 to 1.7 dB compared to SC detection, which suffers no penalty from CD. At low SNR values below 5 dB, SD detection achieves higher capacity per symbol (b/symbol) than KK detection but requires slightly more bandwidth.

Acknowledgment

The authors thank Norman Swenson for illuminating discussions, and Fabio Barbosa and Darli Mello for pointing us to references on estimating mutual information with non-Gaussian noise.

References

[1] E. Ip, A. P. T. Lau, D. J. F. Barros, and J. M. Kahn, "Coherent detection in optical fiber systems," *Opt. Express,*, vol. 16, no. 2, pp. 753–791, Jan. 2008.

[2] J. K. Perin, A. Shastri, and J. M. Kahn, "Coherent data center links," *J. Lightw. Technol.*, vol. 39, no. 3, pp. 730–741, Feb. 2021.

[3] A. Mecozzi, C. Antonelli, and M. Shtaif, "Kramers-Kronig coherent receiver," *Optica*, vol. 3, no. 11, pp. 1220–1227, Nov. 2016.

[4] A. Mecozzi, C. Antonelli, and M. Shtaif, "Kramers-Kronig receivers," *Adv. Opt. Photon.*, vol. 11, no. 3, pp. 480–517, Sep. 2019.

[5] J. J. Maki, "Cloud optics-IEEE 802.3 Ethernet, OIF, and MSA defined optical specifications in data-center aligned form factors," in *Proc. Adv. Photon.*, Zurich, Switzerland, 2018, Paper SpTu3F.1.

[6] A. Li, W.-R. Peng, Y. Cui, and Y. Bai, "80-GBd probabilistic shaped 256QAM transmission over 560-km SSMF enabled by dual-virtual-carrier assisted kramers-kronig detection," in *Proc. Opt. Fiber Commun. Conf.*, San Diego, CA, USA, 2020, Paper M3J.8.

[7] T. Bo and H. Kim, "Coherent versus Kramers-Kronig transceivers in metro applications: A power consumption perspective," in *Proc. Opt. Fiber Comm. Conf.*, San Diego, CA, USA, 2019, Paper M1H.7.

[8] T. Bo and H. Kim, "Kramers-Kronig receiver operable without digital upsampling," *Opt. Express,*, vol. 26, no. 11, pp. 13810–13818, May. 2018.

[9] T. Wang and A. J. Lowery, "Minimum phase conditions in Kramers-Kronig optical receivers," *J. Lightw. Technol.*, vol. 38, no. 22, pp. 6214–6220, Nov. 2020.

[10] A. J. Lowery, T. Wang, and B. Corcoran, "Clipping-enhanced Kramers-Kronig receivers," in *Proc. Opt. Fiber Commun. Conf.*, San Diego, CA, USA, 2019, Paper M1H.2.

[11] A. J. Lowery, T. Wang, and B. Corcoran, "Enhanced Kramers-Kronig single-sideband receivers," *J. Lightw. Technol.*, vol. 38, no. 12, pp. 3229–3237, Jun. 2020.

[12] C. Füllner *et al.*, "Complexity analysis of the Kramers-Kronig receiver," *J. Lightw. Technol.*, vol. 37, no. 17, pp. 4295–4307, Sep. 2019.

[13] Y. Fan, X. Tang, D. Wang, X. Zhang, and L. Xi, "Probabilistic shaping for direct detection transmission with Kramers-Kronig receiver," in *Proc. 18th Int. Conf. Opt. Commun. Netw.*, Huangshan, China, 2019, pp. 1–3.

[14] E. S. Chou, H. Srinivas, and J. M. Kahn, "Phase retrieval-based coherent receivers," in *Proc. Opt. Fiber Commun. Conf.*, 2021, Paper Th5F.1.

[15] X. Chen *et al.*, "Kramers-Kronig receivers for 100-km datacenter interconnects," *J. Lightw. Technol.*, vol. 36, no. 1, pp. 79–89, Jan. 2018.

[16] L. Shu *et al.*, "Single-lane 112-Gbit/s SSB-PAM4 transmission with dual-drive MZM and Kramers-Kronig detection over 80-km SSMF," *IEEE Photon. J.*, vol. 9, no. 6, pp. 1–9, Dec. 2017.

[17] Z. Li *et al.*, "Spectrally efficient 168 Gb/s/λ WDM 64-QAM single-sideband Nyquist-subcarrier modulation with Kramers-Kronig direct-detection receivers," *J. Lightw. Technol.*, vol. 36, no. 6, pp. 1340–1346, Mar. 2018.

[18] Y. Zhu, M. Jiang, X. Ruan, Z. Chen, C. Li, and F. Zhang, "6.4 Tb/s (32 × 200 Gb/s) WDM direct-detection transmission with twin-SSB modulation and Kramers-Kronig receiver," *Opt. Commun.*, vol. 415, pp. 64–69, May. 2018.

[19] F. R. Kschischang and S. Pasupathy, "Optimal nonuniform signaling for Gaussian channels," *IEEE Trans. Inf. Theory*, vol. 39, no. 3, pp. 913–929, May. 1993.

[20] T. M. Cover and J. A. Thomas, *Elements of Information Theory*. New York, NY, USA: Wiley, 2006.

[21] R.-J. Essiambre, G. Kramer, P. J. Winzer, G. J. Foschini, and B. Goebel, "Capacity limits of optical fiber networks," *J. Lightw. Technol.*, vol. 28, no. 4, pp. 662–701, Feb. 2010.

[22] T. Fehenberger, F. Kristl, C. Behrens, A. Ehrhardt, A. Gladisch, and N. Hanik, "Estimates of constrained coded modulation capacity for optical networks," in *Proc. Photon. Netw.; ITG Symp.*, Leipzig, Germany, 2014, pp. 1–6.

[23] S. Hranilovic, "Minimum-bandwidth optical intensity Nyquist pulses," *IEEE Trans. Commun.*, vol. 55, no. 3, pp. 574–583, Mar. 2007.

[24] A. Alvarado, E. Agrell, D. Lavery, R. Maher, and P. Bayvel, "Replacing the soft-decision FEC limit paradigm in the design of optical communication systems," *J. Lightw. Technol.*, vol. 33, no. 20, pp. 4338–4352, Oct. 2015.

[25] J. Cho and P. J. Winzer, "Probabilistic constellation shaping for optical fiber communications," *J. Lightw. Technol.*, vol. 37, no. 6, pp. 1590–1607, Mar. 2019.

[26] D.-S. Shiu, G. J. Foschini, M. J. Gans, and J. M. Kahn, "Fading correlation and its effect on the capacity of multielement antenna systems," *IEEE Trans. Commun.*, vol. 48, no. 3, pp. 502–513, Mar. 2000.

[27] G. Forney, R. Gallager, G. Lang, F. Longstaff, and S. Qureshi, "Efficient modulation for band-limited channels," *IEEE J. Sel. Areas Commun.*, vol. 2, no. 5, pp. 632–647, Sep. 1984.

[28] A. R. Calderbank and L. H. Ozarow, "Nonequiprobable signaling on the Gaussian channel," *IEEE Trans. Inf. Theory*, vol. 36, no. 4, pp. 726–740, Jul. 1990.

[29] D.-S. Shiu and J. M. Kahn, "Shaping and nonequiprobable signaling for intensity-modulated signals," *IEEE Trans. Inf. Theory*, vol. 45, no. 7, pp. 2661–2668, Nov. 1999.

[30] W. Mao and J. M. Kahn, "Lattice codes for amplified direct-detection optical systems," *IEEE Trans. Commun.*, vol. 56, no. 7, pp. 1137–1145, Jul. 2008.

[31] *IEEE Standard for Ethernet Amendment 2: Physical Layer Specifications and Management Parameters for 100 Gb/s Operation Over Backplanes and Copper Cables*, IEEE Standard 802.3bj, Sep. 2014.

[32] S. Arimoto, "An algorithm for computing the capacity of arbitrary discrete memoryless channels," *IEEE Trans. Inf. Theory*, vol. 18, no. 1, pp. 14–20, Jan. 1972.

[33] K.-P. Ho, "Exact evaluation of the capacity for intensity-modulated direct-detection channels with optical amplifier noises," *IEEE Photon. Technol. Lett.*, vol. 17, no. 4, pp. 858–860, Apr. 2005.

[34] T. Bo, R. Deng, J. He, and H. Kim, "On the hardware complexity of Kramers-Kronig receiver," in *Proc. Conf. Lasers Electro-Opt. Pacific Rim*, Hong Kong, China, 2018, Paper Tu2I.2.

[35] S. T. Le *et al.*, "1.72-Tb/s virtual-carrier-assisted direct-detection transmission over 200 km," *J. Lightw. Technol.*, vol. 36, no. 6, pp. 1347–1353, Mar. 2018.

[36] C. Antonelli, A. Mecozzi, M. Shtaif, X. Chen, S. Chandrasekhar, and P. J. Winzer, "Polarization multiplexing with the Kramers-Kronig receiver," *J. Lightw. Technol.*, vol. 35, no. 24, pp. 5418–5424, Dec. 2017.

[37] T. M. Hoang *et al.*, "Single wavelength 480 Gb/s direct detection over 80 km SSMF enabled by stokes vector Kramers Kronig transceiver," *Opt. Express,*, vol. 25, no. 26, pp. 33534–33542, Dec. 2017.

Elaine S. Chou received the B.S.E. degree in electrical engineering from Princeton University, Princeton, NJ, USA, in 2016 and the M.S. and Ph.D. degrees in electrical engineering from Stanford University, Stanford, CA, USA, in 2018 and 2021, respectively. Her research interests include optical fiber communications, modulation and coding techniques, and signal processing.

Hrishikesh Srinivas (Graduate Student Member, IEEE) received the B.E. degree in photonic engineering and the B.Sc. degree in mathematics and physical science from the University of New South Wales, Sydney, NSW, Australia, in 2017, and the M.S. degree in electrical engineering from Stanford University, Stanford, CA, USA, in 2019, where he is currently working toward the Ph.D. degree. His current research interests include optical fiber communications, optical amplifier physics, and photonics.

Joseph M. Kahn (Fellow, IEEE) received the A.B., M.A., and Ph.D. degrees in physics from the University of California, Berkeley, Berkeley, CA, USA, in 1981, 1983, and 1986, respectively. In 1987–1990, he was with AT&T Bell Laboratories. In 1989, he demonstrated the first successful synchronous (i.e., coherent) detection using semiconductor lasers achieving record receiver sensitivity. Between 1990–2003, he was on the Electrical Engineering and Computer Sciences Faculty, Berkeley. He demonstrated coherent detection of QPSK in 1992. In 1999, along with D.-S. Shiu, authored and coauthored the first work on probabilistic shaping for optical communications. In the 1990s and early 2000s, he and collaborators performed seminal work on indoor and outdoor free-space optical communications and multi-input multi-output wireless communications. In 2000, he and K.-P. Ho founded StrataLight Communications, whose 40 Gb/s-per-wavelength long-haul fiber transmission systems were deployed widely by AT&T, Deutsche Telekom, and other carriers. In 2002, Ho and he applied to patent the first electronic compensation of fiber Kerr nonlinearity. StrataLight was acquired by Opnext in 2009. In 2003, he became a Professor of electrical engineering with the E. L. Ginzton Laboratory, Stanford University, Stanford, CA, USA. He and his collaborators have extensively studied rate-adaptive coding and modulation, as well as digital signal processing for mitigating linear and nonlinear impairments in coherent systems. In 2008, E. Ip and he (and G. Li independently) invented simplified digital backpropagation for compensating fiber Kerr nonlinearity and dispersion. Since 2004, he and his collaborators have studied propagation, modal statistics, spatial multiplexing, and imaging in multimode fibers, elucidating principal modes, and demonstrating transmission beyond the traditional bandwidth-distance limit in 2005, deriving the statistics of coupled modal group delays and gains in 2011, and deriving resolution limits for imaging in 2013. His current research addresses optical frequency comb generators, coherent data center links, rate-adaptive access networks, fiber Kerr nonlinearity mitigation, ultralong-haul submarine links, and optimal free-space transmission through atmospheric turbulence. He was the recipient of the National Science Foundation Presidential Young Investigator Award in 1991.